Cdc42 promotes transendothelial migration of cancer cells through β1 integrin

Nicolas Reymond,[1] Jae Hong Im,[2] Ritu Garg,[1] Francisco M. Vega,[1] Barbara Borda d'Agua,[1] Philippe Riou,[1] Susan Cox,[1] Ferran Valderrama,[1] Ruth J. Muschel,[2] and Anne J. Ridley[1]

[1]Randall Division of Cell and Molecular Biophysics, King's College London, London SE1 1UL, England, UK
[2]Gray Institute for Radiation Oncology and Biology, University of Oxford, Oxford OX3 7LJ, England, UK

Cancer cells interact with endothelial cells during the process of metastatic spreading. Here, we use a small interfering RNA screen targeting Rho GTPases in cancer cells to identify Cdc42 as a critical regulator of cancer cell–endothelial cell interactions and transendothelial migration. We find that Cdc42 regulates β1 integrin expression at the transcriptional level via the transcription factor serum response factor (SRF). β1 integrin is the main target for Cdc42-mediating interaction of cancer cells with endothelial cells and the underlying extracellular matrix, as exogenous β1 integrin expression was sufficient to rescue the Cdc42-silencing phenotype. We show that Cdc42 was required in vivo for cancer cell spreading and protrusion extension along blood vessels and retention in the lungs. Interestingly, transient Cdc42 depletion was sufficient to decrease experimental lung metastases, which suggests that its role in endothelial attachment is important for metastasis. By identifying β1 integrin as a transcriptional target of Cdc42, our results provide new insight into Cdc42 function.

Introduction

Cancer progression and metastasis are dependent on changes in cancer cell adhesion and migration. To form metastases, cells that have detached from a primary tumor first invade the surrounding tissues (Friedl and Alexander, 2011). Cells then enter the circulation either through the lymph or by migrating directly through blood vessel walls (intravasation), and disseminate throughout the body via the blood before adhering to endothelial cells (ECs) lining the microvasculature (Madsen and Sahai, 2010). Depending on the cancer origin and the target organ, tumor cells display different metastatic behaviors. They can initially proliferate in blood vessels and then extravasate (Al-Mehdi et al., 2000), or can directly extravasate as single cells and then invade into the tissues (Gassmann et al., 2009; Martin et al., 2010). To form secondary tumors, they then need to survive and proliferate in this new environment (Joyce and Pollard, 2009; Nguyen et al., 2009). Both cell–cell adhesion molecules and chemokines, as well as their receptors, can contribute to metastasis (Joyce and Pollard, 2009; Madsen and Sahai, 2010).

Rho family GTPases play a central role in cell migration and invasion by coordinately regulating cytoskeletal dynamics and turnover of cell–cell and cell–ECM adhesions (Vega and Ridley, 2008; Ridley, 2011). They predominantly act on membranes and affect membrane dynamics by regulating actin polymerization. So far, 20 Rho family members have been identified in humans (Vega and Ridley, 2007). The expression level of several Rho GTPases is frequently altered in tumors and metastases, and this often correlates with poor prognosis (Kusama et al., 2006; Vega and Ridley, 2008). Several Rho GTPases or their targets have been specifically implicated in the metastatic process in animal models for cancer progression, including RhoC, Rho kinases, and PAKs, although the steps of metastasis that they regulate have not been defined precisely (Hall, 2009).

Here, we identify Cdc42 as a key regulator of cancer cell transendothelial migration (TEM) in a Rho GTPase RNAi

Correspondence to Anne J. Ridley: anne.ridley@kcl.ac.uk

F.M. Vega's present address is Seville Institute for Biomedicine, Universidad de Sevilla, 41013 Sevilla, Spain.

P. Riou's present address is Cancer Research UK, London Research Institute, Lincoln's Inn Fields Laboratories, London WC2A 3LY, England UK.

F. Valderrama's present address is Division of Basic Medical Science, St. George's, University of London, London SW17 0RE, England UK.

Abbreviations used in this paper: CFSE, 5-(and-6)-carboxyfluorescein diacetate succinimidyl ester; EC, endothelial cell; HUVEC, human umbilical vein endothelial cell; MAL, megakaryoblastic leukemia 1; PE, phycoerythrin; SCID, severe combined immunodeficiency; SRF, serum response factor; TEM, transendothelial migration.

The Rockefeller University Press $30.00
J. Cell Biol. Vol. 199 No. 4 653–668
www.jcb.org/cgi/doi/10.1083/jcb.201205169

screen. We demonstrate that Cdc42 regulates β1 integrin at the transcriptional level via serum response factor (SRF), and that this is the major mechanism whereby Cdc42 regulates cancer cell TEM. We find that transient Cdc42 depletion is sufficient to decrease early cancer cell colonization in the lungs and to inhibit experimental metastasis formation in vivo. Our results indicate that targeting the early steps of cancer cell interaction with ECs could inhibit metastasis.

Results

Effects of Rho GTPases on cancer cell adhesion to ECs

During TEM, cancer cells first adhere to ECs, open EC junctions, induce endothelial retraction, and then insert into the endothelial monolayer between ECs, a process we name intercalation (Reymond et al., 2012). Of the cancer cell lines we tested (see Table S1), PC3 and DU145 prostate cancer cells and MDA-MB-231 breast cancer cells showed the highest level of adhesion and intercalation and thus were used in our experiments.

An siRNA screen was performed to determine which Rho GTPases affect cancer cell adhesion to ECs. PC3 cells were used for this screen because they express all 20 Rho GTPase genes, whereas DU145 and MDA-MB-231 cells do not (unpublished data). siRNA pools targeting RhoA, RhoC, Rac1, Rac3, Cdc42, Rnd2, RhoH, and RhoBTB1 significantly reduced adhesion by >25%, whereas RhoQ depletion increased adhesion by 45% compared with control cells (Fig. 1 A). Two different single siRNAs similarly reduced adhesion for Cdc42, Rac1, and RhoA (Fig. 1 B). Cdc42, Rac1, and RhoA depletion also reduced adhesion of DU145 cells to ECs (Fig. 1 C).

Cdc42 depletion strongly impairs intercalation

To investigate whether the reduced adhesion of Rho GTPase–depleted cells to ECs affected subsequent PC3 cell intercalation, we monitored cells by time-lapse microscopy (Fig. 2 A and Video 1). These experiments showed that Cdc42-depleted cancer cells had the strongest delay in intercalation of the adhesion screen hits that we tested (Fig. 2 B, Video 1, and not depicted). Approximately 50% of Cdc42-depleted PC3 and DU145 cells had still not intercalated by 300 min (Fig. 2 B and Fig. S1 B). Similarly, Cdc42 depletion in MDA-MB-231 cells strongly inhibited intercalation (Fig. S1 C). Rac1- and RhoA-depleted PC3 and DU145 cells showed a delay in intercalation, but by 300 min they had caught up with control cells (Fig. 2 B). Depletion of other tested Rho GTPases similarly delayed intercalation or had no effect (unpublished data). The effects of Cdc42, Rac1, and RhoA depletion on PC3 cell intercalation were rescued by expression of siRNA-resistant cDNAs (Fig. 2 C and Fig. S2). Cdc42-depleted cells crawled a longer distance on ECs, reflecting their reduced intercalation (Fig. 2 D; note that cells that did not intercalate were included). Cdc42 therefore regulates both cancer cell adhesion and intercalation, whereas other Rho GTPases contribute to cancer cell adhesion but do not have a long-term effect on intercalation. We therefore decided to characterize the function of Cdc42 during cancer cell TEM, comparing with Rac1 and RhoA as examples of Rho GTPases that have a similar effect to Cdc42 on adhesion to ECs but do not strongly alter intercalation.

Cdc42, Rac1, and RhoA have similar effects on EC junction opening

We next aimed to identify the steps of the TEM process specifically regulated by Cdc42. We first analyzed how Cdc42, Rac1, and RhoA affect endothelial junction opening. By 30 min after addition to ECs, most control PC3 cells had reached cell–cell junctions and started to induce localized gaps between ECs directly underneath or near their site of adhesion, identified by the local disappearance of the adherens junction proteins β-catenin (Fig. 3 A) and VE-cadherin (not depicted). Cells first extend protrusions across the endothelial surface, toward EC junctions, which then induce localized gaps followed by their progressive opening (Fig. S1 A). By 60 min, many had induced endothelial retraction and spread between ECs (Fig. 3 A). At these time points, Cdc42-, Rac1-, and RhoA-depleted cells were less frequently localized on top of an EC junction compared with control cells (Fig. 3, A and B), which suggests that they move more slowly to these sites. Indeed, time-lapse microscopy tracking showed they moved ∼30% slower on ECs (not depicted). Moreover, when they were localized on top of a junction, fewer cells induced the local disappearance of junctional proteins or formation of intercellular gaps (Fig. 3, A and C). Altogether these data show that Cdc42, Rac1, and RhoA depletion all delay EC junction opening, which suggests that this is due to reduced initial adhesion, which they all affect similarly (Fig. 1). Cdc42-specific functions required for intercalation therefore are likely to occur at a later stage of TEM.

Cdc42 regulates cancer cell interactions with the subendothelial ECM

After junctional opening, cancer cells interact with the ECM underlying the ECs in order to spread and intercalate between ECs (Reymond et al., 2012). We therefore investigated whether Cdc42 selectively affects this step of TEM. Analysis of movies showed that control cancer cells first extended multiple dynamic protrusions on top of the EC toward junctions, and subsequently on the ECM underlying a gap between ECs, then rapidly flattened out and spread by inducing retraction of neighboring ECs (Video 2). Intercalated cancer cells moved within the EC monolayer, eventually leading to gaps between ECs. In contrast, the Cdc42-depleted cells that did intercalate were taller than control, RhoA-depleted, or Rac1-depleted cells because they did not spread and their nuclei remained above the monolayer (Fig. 4 A and not depicted). Movies of Cdc42-depleted cells showed that they extended protrusions in all directions but did not spread or integrate into the EC monolayer efficiently (Fig. 4 B and Video 2). Rac1- and RhoA-depleted cells did not show this behavior. This suggests that Cdc42 but not Rac1 or RhoA mediates cancer cell interactions with the subendothelial ECM. Indeed, Cdc42-depleted cells showed a similar behavior when attaching to ECM proteins:

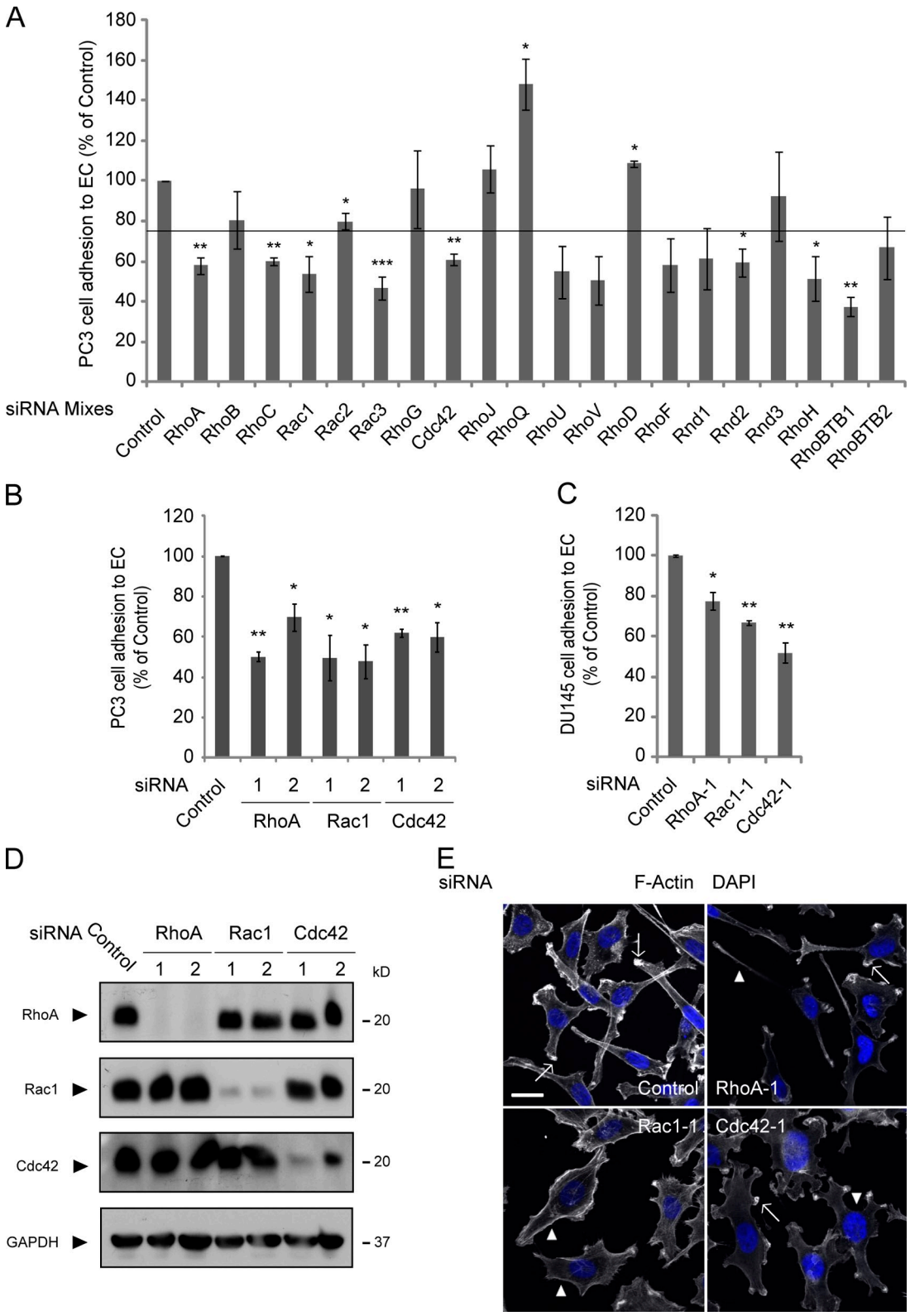

Figure 1. **Several Rho GTPases regulate cancer cell adhesion to ECs.** (A and B) PC3 cells transfected with the indicated siRNA pools (A) or single siRNAs (B) were added to HUVECs for 15 min, and the percentage adhesion relative to control was determined. Data are expressed as the percentage of total cells analyzed. (C) DU145 cells transfected with siRNAs targeting Cdc42, Rac1, and RhoA or control siRNA (control) were added to confluent HUVECs for 30 min, and the number of cells adhering to ECs was scored. Data are presented as percentages with respect to control cells. (D) Lysates of PC3 cells transfected with indicated single siRNAs were immunoblotted as shown. Values (A–C) are means ± SEM (error bars; $n \geq 3$); ***, $P < 0.001$; **, $P < 0.01$; *, $P < 0.05$. (E) Confocal images of PC3 cells transfected with single siRNAs as indicated. Cells were fixed and stained with DAPI (blue) and for F-actin (grayscale). Arrows indicate F-actin–rich protrusions (control, RhoA, Cdc42); arrowheads indicate an elongated tail (RhoA), cells with no F-actin-rich protrusions (Rac1), or an area of membrane retraction between F-actin–rich protrusions (Cdc42). Bar, 20 µm.

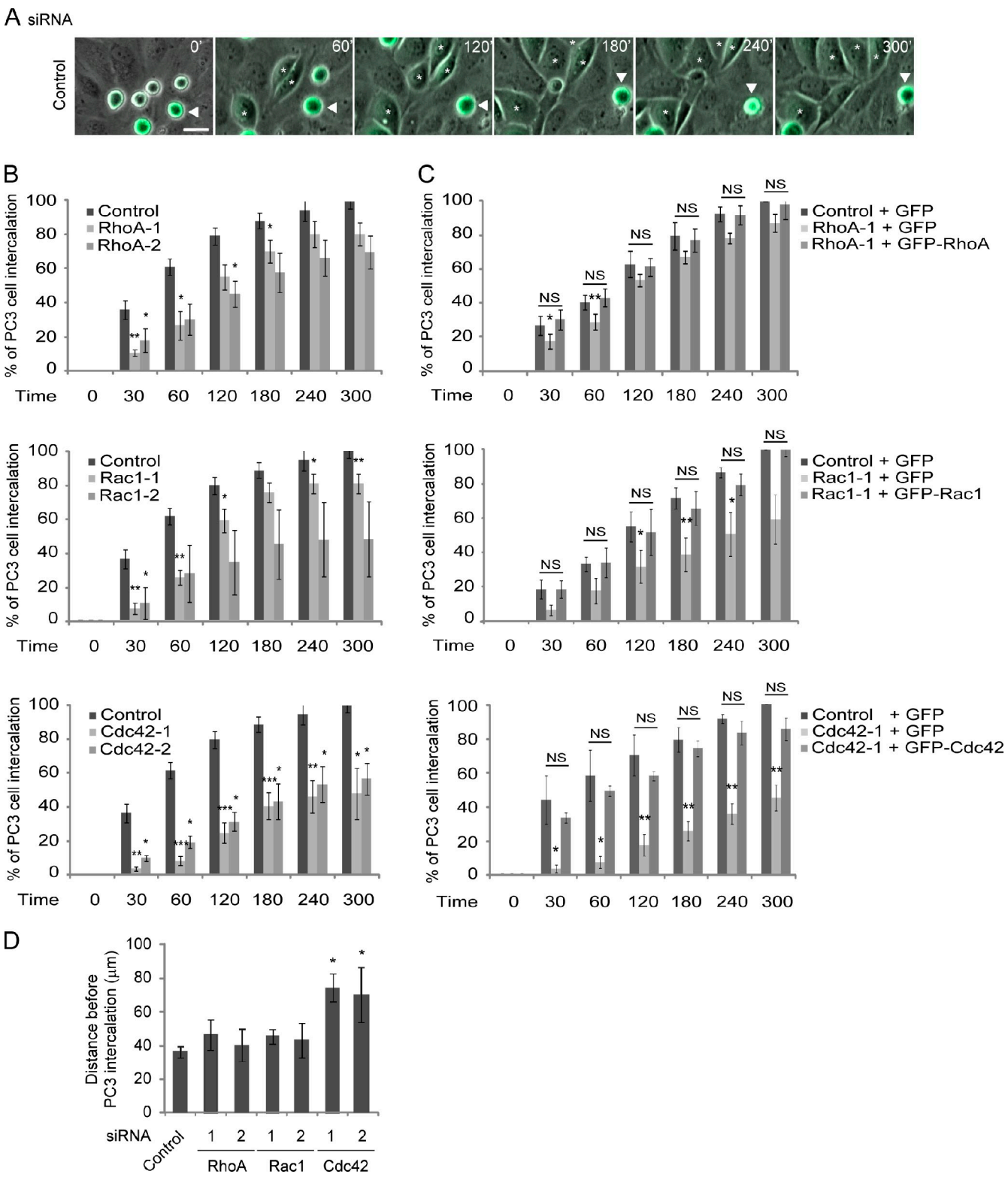

Figure 2. **Cdc42 depletion inhibits cancer cell intercalation between ECs.** (A) CFSE-labeled PC3 cells transfected with control siRNA were filmed for 300 min on HUVECs. Asterisks mark PC3 cells that intercalate; arrowheads indicate a cell that does not intercalate. Bar, 50 µm. (B and C) Graphs show time of intercalation for individual cells. Cells were filmed on HUVECs for 300 min. In each experiment, ≥100 cells were analyzed in at least three fields. Data are expressed as the percentage of total cells. (B) PC3 cells transfected with the indicated siRNAs. (C) PC3 cells transfected with the indicated siRNAs were transfected after 48 h with siRNA-resistant-cDNAs encoding GFP-tagged Cdc42, Rac1, and RhoA, respectively. (D) Distance migrated on top of ECs before intercalation. Data are expressed as the percentage of control cells. Values (B–D) are means ± SEM (error bars; $n \geq 3$); ***, $P < 0.001$; **, $P < 0.01$; *, $P < 0.05$.

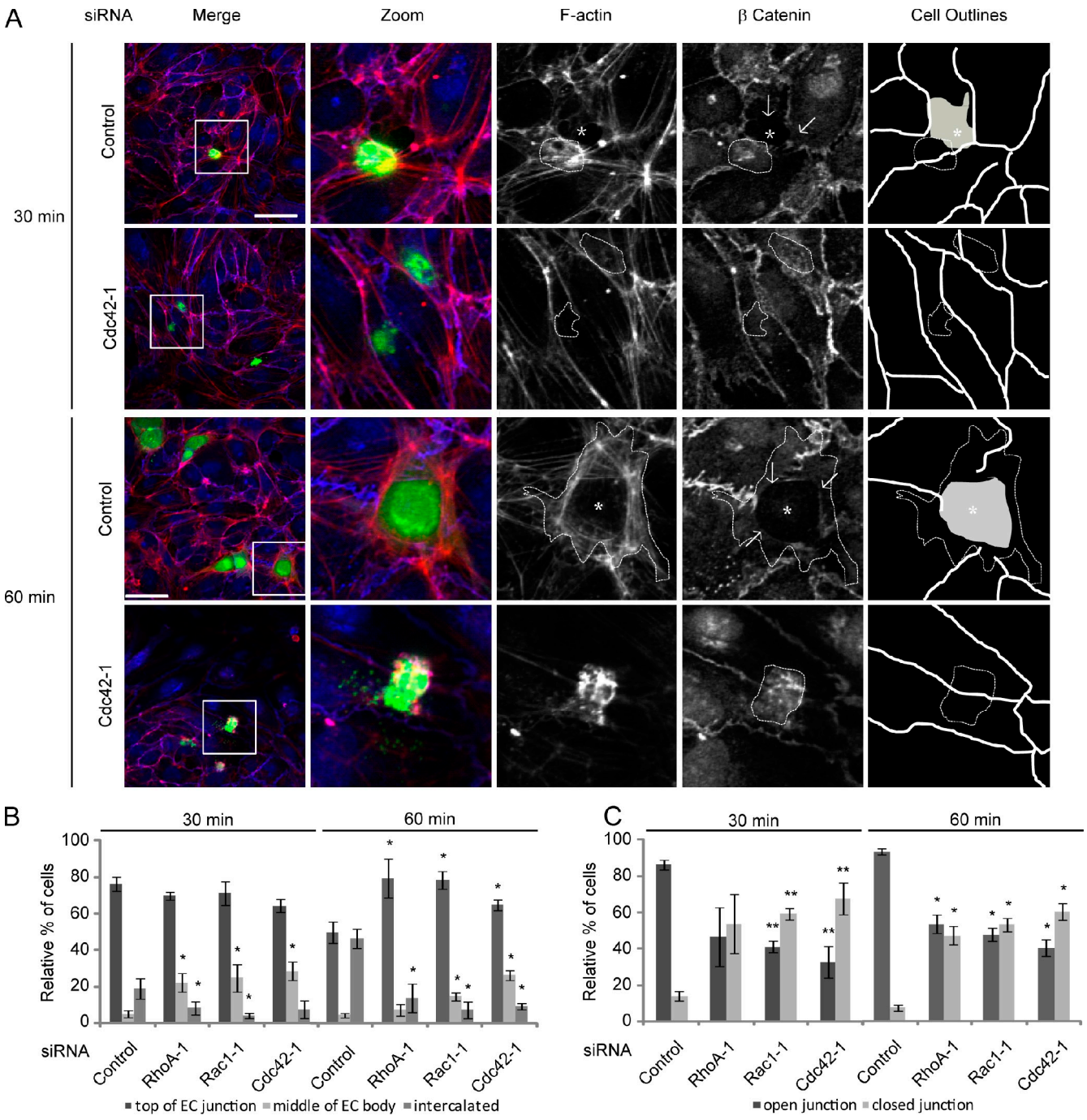

Figure 3. **Cdc42, Rac1, and RhoA depletion inhibits EC junctional opening.** (A) CFSE-labeled PC3 cells were added to HUVECs for 30 and 60 min, then stained for β-catenin and F-actin. Cell outlines are shown. A gap in the endothelial monolayer by the control PC3 cell is outlined and marked with an asterisk. Arrows show the disappearance of β-catenin. Bar, 50 µm. (B and C) Quantification of sites of cancer cell adhesion with respect to EC junctions and the status of EC junctions near cancer cell adhesion sites. Data are expressed as the percentage of total cells analyzed; ≥50 cells/experiment. Values are means ± SEM (error bars; $n \geq 3$); ***, $P < 0.001$; **, $P < 0.01$; *, $P < 0.05$.

they extended small protrusions in multiple directions and had defective spreading compared with control cells, which spread quite uniformly by extending lamellipodia around the periphery (Fig. 4, C and D; and Video 3). Cdc42-depleted but not RhoA- or Rac1-depleted cells also showed reduced adhesion to fibronectin, Matrigel, or uncoated plastic (Fig. 4, E and F; and not depicted). In addition to lamellipodia, cells can generate highly dynamic plasma membrane protrusions known as blebs (Charras and Paluch, 2008). We observed that a proportion of Cdc42-depleted PC3 cells blebbed for long periods after adhesion (Fig. 4 D, bottom), presumably reflecting their reduced adhesion so that they are "trapped" in an early stage of spreading (Dubin-Thaler et al., 2008; Norman et al., 2010). These cells were not apoptotic because they eventually spread, and we did not observe any decrease in viability of Cdc42-depleted cells (unpublished data). Our observations together indicate

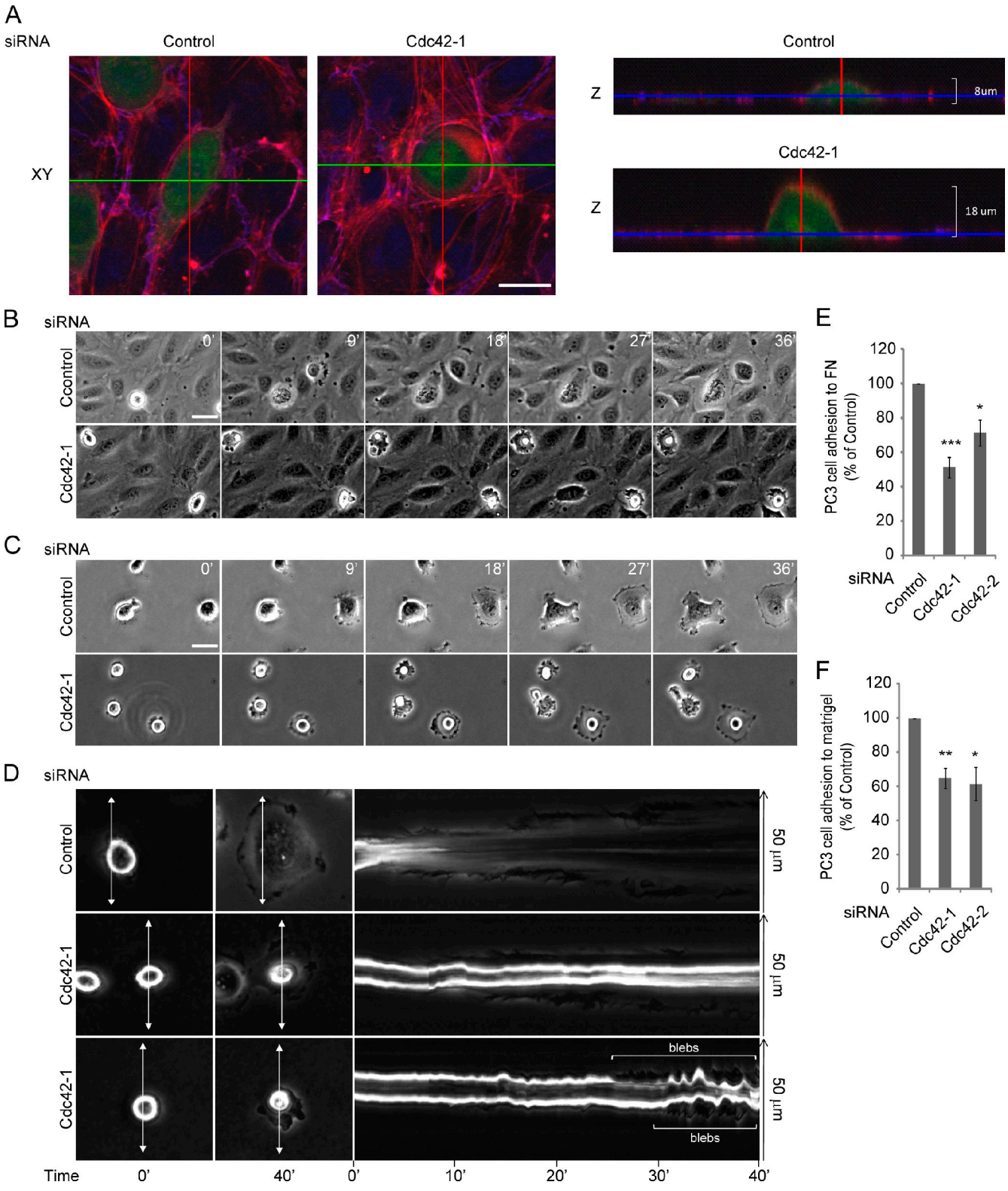

Figure 4. **Cdc42 depletion specifically reduces cancer cell adhesion and spreading to ECM.** PC3 cells were transfected with the indicated siRNAs. (A) Confocal stack images of PC3 cells labeled with CFSE (green) and added to HUVECs for 4 h. Cells were stained with DAPI (blue) and for F-actin (red). Z views show cell height. Bar, 18 µm. (B) Time-lapse stills (Video 2) of PC3 cells on ECs. Bar, 50 µm. (C) Time-lapse stills (Video 3) of PC3 cells on fibronectin. Bar, 50 µm. (D) Kymographs (right panels) from time-lapse movies of cells plated on fibronectin. First and last images of time-lapse movies are shown (left panels); arrows represent where the kymographs were made. Blebbing regions are indicated with white brackets (bottom right panel). Cell adhesion to fibronectin- (E) or Matrigel-coated (F) dishes at 15 min. Data (E and F) are expressed as the percentage of control cells. Values are means ± SEM (error bars; $n \geq 3$); ***, $P < 0.001$; **, $P < 0.01$; *, $P < 0.05$.

that Cdc42-depleted cells have a strong defect in adhesion to ECM that inhibits intercalation.

To determine whether Cdc42 affected the whole TEM process, we used a 3D assay in which ECs were grown on a thick collagen I layer (Cain et al., 2011). Cdc42 depletion strongly inhibited extravasation of MDA-MB-231 cells: at 6 h, >50% of Cdc42-depleted cells remained rounded on top of ECs, whereas control cells had intercalated and started to invade the ECM underneath ECs (Fig. S1, D and E).

Cdc42 is required for the spreading and colonization of cancer cells in the lung vasculature in vivo

Because Cdc42 depletion reduced all the steps of TEM in vitro, we investigated whether Cdc42 affected the interactions of cancer cells with vascular ECs in mouse lungs in vivo. YFP control and CFP-Cdc42–depleted PC3 cells were coinjected in the vena cava or in the tail vein 72 h after siRNA transfection to allow the behavior of Cdc42-depleted cells to be compared with control cells at the same time and in the same animal. EC lining blood vessels were stained by injecting a phycoerythrin (PE)-labeled anti–PECAM-1 antibody. At different time points after injection (10 min, 6 h, or 24 h), the lung–heart complex was isolated, inflated, and analyzed by confocal microscopy, as described previously (Im et al., 2004).

We observed that 90% of YFP-PC3 control cells already had one or multiple cell protrusions extending along the vessels at 10 min after injection. This phenotype was maintained at 6 and 24 h. At these time-points, very few had extravasated (Fig. 5, A and B; and Video 4), which is consistent with previous observations using other cancer cell types (Al-Mehdi et al., 2000). In contrast to control cells, most CFP-Cdc42–depleted cells did not extend protrusions and remained round or displayed a tubular vessel shape indicating that they had reduced interaction with the endothelium (Fig. 5, A and B; and Video 5). Similar results were obtained using CFP control cells and YFP-PC3 Cdc42-depleted cells (Fig. S3, A and B). To study the interaction of cancer cells with ECs in more detail, we analyzed the localization of endothelial PECAM-1 around cancer cells in the lung blood vessels (Fig. S3 C). PECAM-1 staining was higher around Cdc42-depleted cells than control cells, which suggests that control cancer cells but not Cdc42-depleted cells had displaced ECs and started to intercalate in vivo, or, alternatively, that control cells were more strongly attached to the endothelium and thereby prevented access of PECAM-1 antibodies. Altogether, we show for the first time that Cdc42 is required for spreading of cancer cells in blood vessels in vivo.

In the lungs, cancer cell death is high during the first 24 h in the lung vasculature (up to 99% of injected cells; Mehlen and Puisieux, 2006). We therefore investigated whether Cdc42 depletion affected early colonization of PC3 cells in the lungs. In vitro, Cdc42 depletion did not detectably affect cell proliferation over 3 d (unpublished data). We quantified the ratio between YFP-PC3 control cells and CFP-Cdc42–depleted PC3 cells during the first 24 h after injection in the tail vein or vena cava. At 10 min, the ratio of YFP cells/CFP cells was 50:50, showing that we injected the same number of each cell population, whereas at 6 h the ratio was 60:40, and at 24 h it was 80:20 (Fig. 5 C). Our results strongly suggest that the defect in spreading of Cdc42-depleted cells to ECs leads to a decrease in early lung colonization.

Transient Cdc42 depletion reduces metastasis formation in vivo

The requirement for Cdc42 in initial cancer cell interaction with the lung endothelium could affect subsequent formation of metastases. To investigate this possibility, we injected Cdc42-depleted PC3 cells or control cells in the tail vein. By using transient Cdc42 depletion and injecting the cells 3 d after siRNA transfection, we were able to specifically target Cdc42-regulated events happening during the first few days after the injection of the cells, as Cdc42 expression is knocked down very efficiently at 3 d after siRNA transfection and returns to normal levels between 6 and 10 d after transfection (Fig. S3 D).

Mice injected with Cdc42-depleted PC3 cells developed significantly less metastatic foci on the surface of lungs than control siRNA-transfected cells (Fig. 5, D and E). The foci were categorized based on size: for all the size categories we observed a decrease in the number of foci when Cdc42 had been depleted (not depicted). In addition, whereas almost all the mice injected with control cells developed metastatic foci on the rib cage, there were no foci on the rib cage in any mice injected with Cdc42-depleted cells (Fig. S3 E). To determine whether Cdc42 affected metastasis formation for another cell type, we injected mice with Cdc42-depleted MDA-MB-231 cells. Although MDA-MB-231 cells formed few lung surface metastatic foci compared with PC3 cells, Cdc42 depletion led to a marked reduction in foci in sections through the lungs (Fig. 6, A and B). Interestingly, we observed that PC3 cells rarely formed foci inside the lungs; nearly all foci were near the surface (unpublished data). Because Cdc42 expression is only transiently reduced for a few days and does not seem to affect cell division in vitro, this strong inhibition of metastasis formation suggests that targeting the interaction of cancer cells with the endothelium through Cdc42 depletion is sufficient to reduce experimental metastasis in vivo.

Cdc42 regulates β1 integrin levels and localization

To investigate the molecular basis for the defects of adhesion and spreading on ECs and the subendothelial ECM observed after Cdc42 depletion, we investigated whether Cdc42 affected integrin levels. Integrins are a large family of heterodimeric cell adhesion molecules involved in the interactions between cells and the ECM and between different cell types, for example, leukocytes and ECs (Humphries, 2000). Using flow cytometry, we confirmed that PC3 cells express β1, β3, and β4 but not β2 integrins (not depicted), as reported previously (Liu, 2000). We observed a significant decrease in cell surface levels of β1 integrin in Cdc42-depleted cells compared with control cells, whereas surface levels of β2, β3, and β4 integrins were not altered (Fig. 7 A and not depicted).

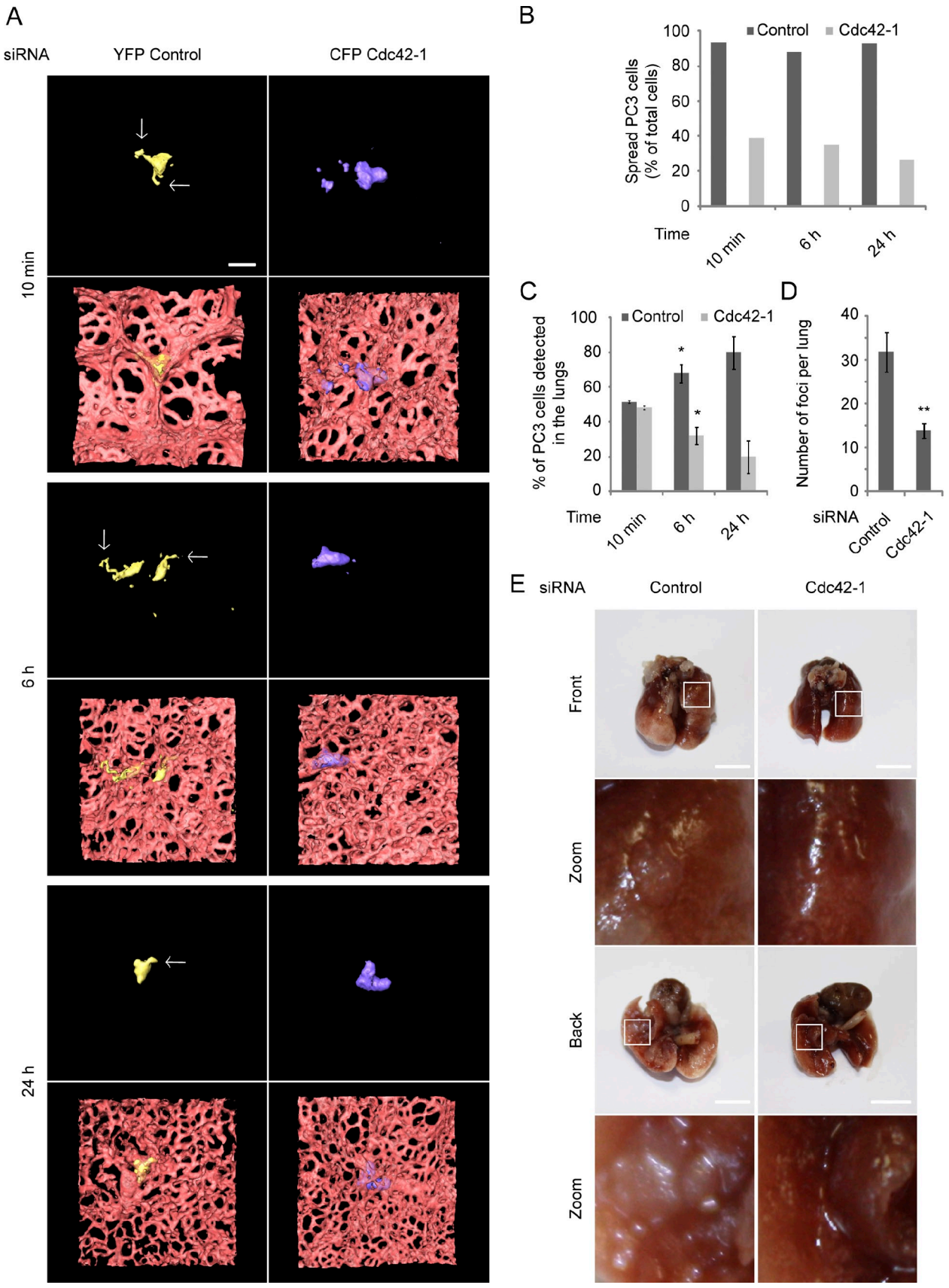

Figure 5. **Cdc42 regulates PC3 cancer cell spreading on lung vascular ECs, retention in the lungs, and metastasis formation in vivo.** CFP-PC3 cells transfected with Cdc42 siRNA and YFP-PC3 cells transfected with control siRNA were coinjected into mice. (A) 3D reconstructions of representative confocal 3D stacks of cells in the lung vasculature. Arrows indicate cancer cell protrusions along the vessels. Bar, 20 µm. (B) Quantification of spread cells in the lung

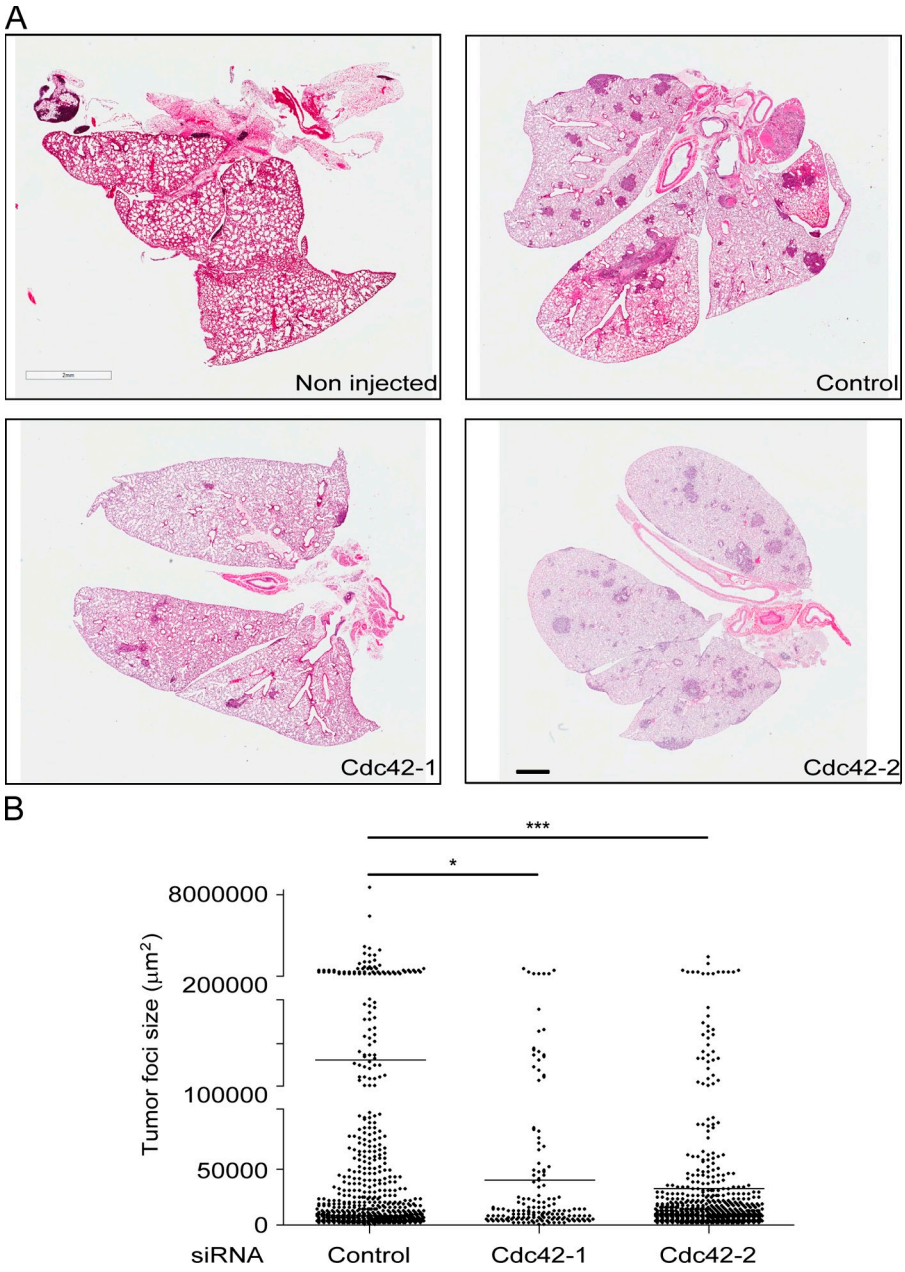

Figure 6. **Transient Cdc42 depletion reduces MDA-MB-231 cell metastasis in vivo.** SCID mice were injected in the tail vein with MDA-MB-231 cells transfected with a control siRNA (Control) or with Cdc42-1 and Cdc42-2 siRNAs. (A) Representative images of whole lung sections stained with hematoxylin and eosin. Bar, 20 mm. (B) Quantification of the percentage of lung areas positive for foci. Values are means ± SEM (error bars); *, $P < 0.05$; ***, $P < 0.001$; determined by a two-way ANOVA test.

A similar decrease in surface β1 integrin was sufficient to impair cell adhesion to ECM (Margadant et al., 2012). Rac1, RhoA, or RhoQ knockdown did not alter β1 integrin levels (unpublished data). The total level of β1 integrin was also decreased by Cdc42 depletion in PC3, DU145, and MDA-MB-231 cells, as determined by immunoblotting and immunofluorescence (Fig. 7, B and C; and Fig. S4, A–C; note that the upper β1 integrin band on blots is the mature cell surface glycosylated protein, and that the lower band is the cytosolic precursor; unpublished data; Isaji et al., 2009). Active β1 integrin levels were similarly decreased in Cdc42-depleted cells, as determined by immunostaining with the 12G10 antibody (not depicted). Interestingly, the protein levels of β1 integrin returned to normal levels 6 d after Cdc42 depletion, following a time course similar to Cdc42 levels (Fig. S3 D). β1 integrin normally localized to actin-rich protrusions of

vasculature. At least 50 single cells per condition were analyzed from at least three independent experiments. Data are expressed as the percentage of the total number of cells analyzed. (C) Number of cells in the lungs. 60 random independent fields were analyzed and the cell number was scored from three independent experiments. Data are expressed as the percentage of total cells analyzed. Values are means ± SEM (error bars); *, $P < 0.05$. (D) Effects of Cdc42 depletion on experimental metastasis formation. Mice were injected intravenously with PC3 cells transfected with control siRNA or Cdc42 siRNA. Quantification of metastatic foci on the lung surface (8 mice for control, 6 mice for Cdc42 siRNA). Values are means ± SEM (error bars); **, $P < 0.01$. (E) Representative images of lungs from mice injected with Cdc42-depleted cells (right) or control siRNA-transfected cells (left). Boxed regions are shown at higher magnification (bottom). Bars, 10 mm.

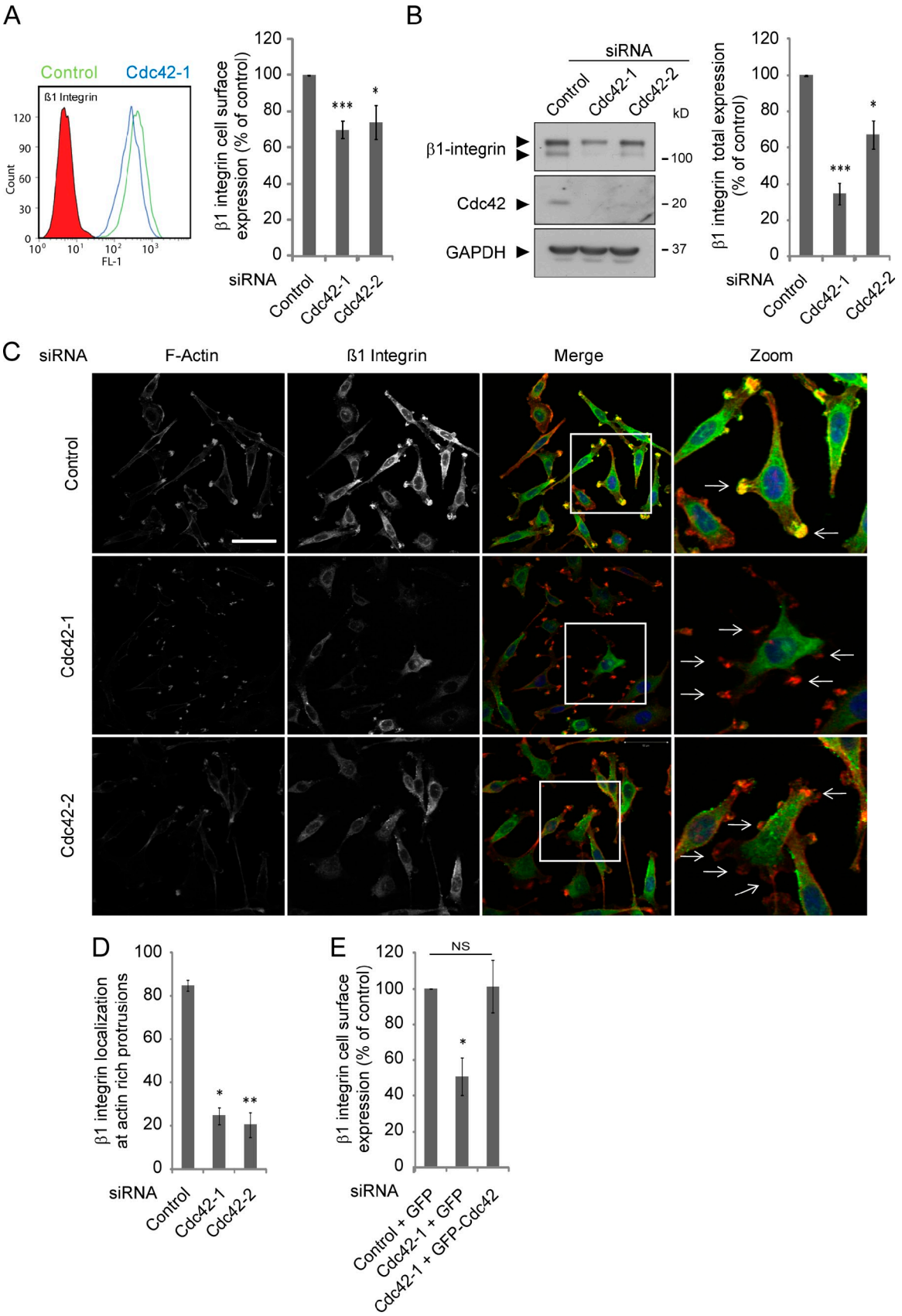

Figure 7. **Cdc42 regulates β1 integrin expression levels.** PC3 cells were transfected with the indicated siRNAs. (A) FACS analysis for β1 integrin. A representative FACS histogram (left) and quantification of FACS analyses (right) are shown; $n \geq 3$. (B) Cell lysates were immunoblotted for Cdc42, β1 integrin, and GAPDH expression. A representative blot is shown (left), as is a quantification of three independent blots for β1 integrin (right). (C) Representative images of cells fixed and stained with DAPI (blue), for F-actin (red) and β1 integrin (green). Arrows indicate actin-rich protrusions. Boxed regions

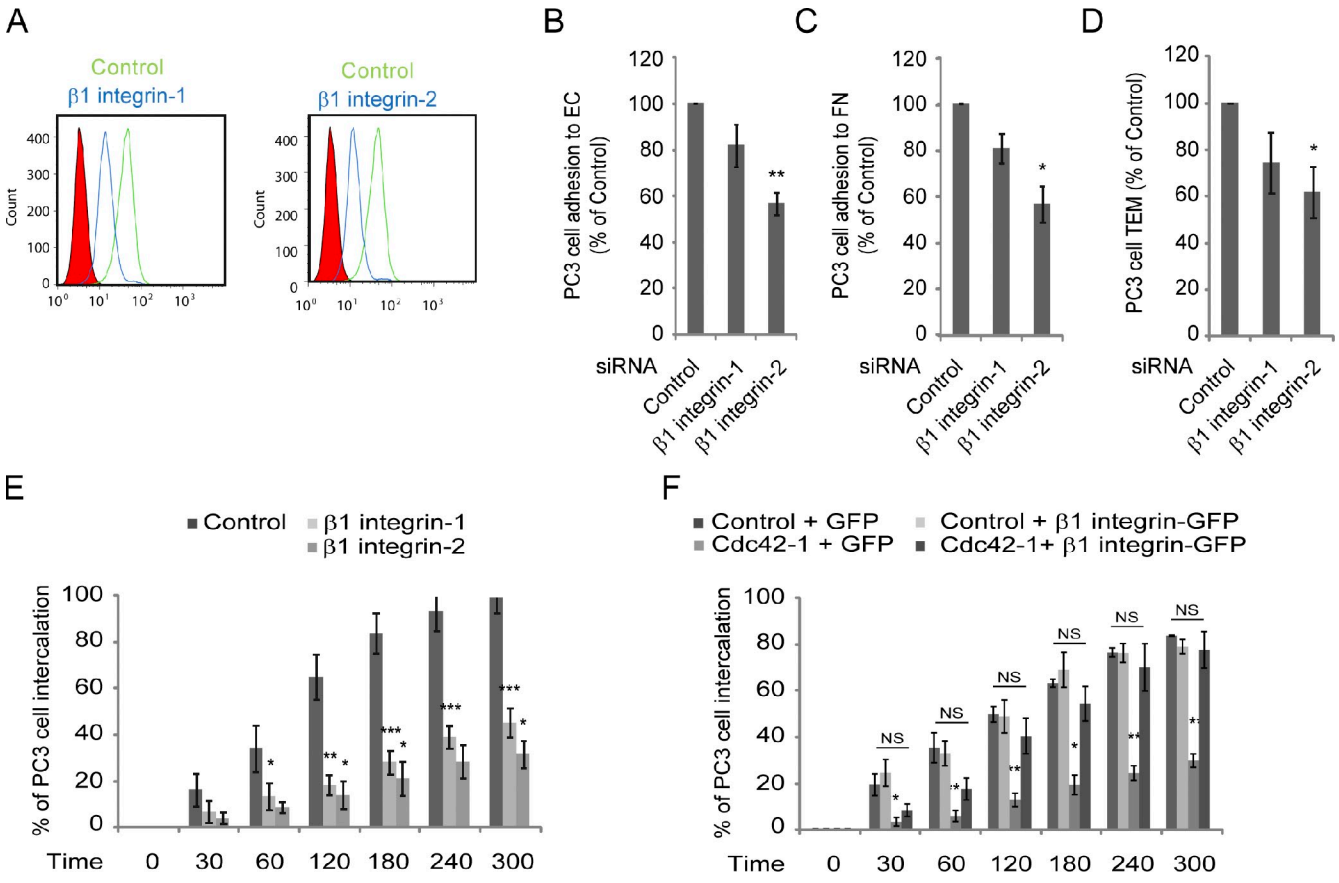

Figure 8. **β1 integrin regulates cancer cell interaction with ECs.** PC3 cells were transfected with the indicated siRNAs. (A) β1 integrin levels were analyzed by FACS. (B–D) Shown is the number of adherent cells on HUVECs (B) or fibronectin-coated dishes (C) for 15 min (D) TEM of PC3 cells. (E and F) Time of intercalation for individual cells. Values (B–F) are means ± SEM expressed as the percentage of the total number of cells ($n \geq 3$); *, $P < 0.05$; **, $P < 0.01$; ***, $P < 0.001$; See also Fig. S7.

PC3 cells, but in Cdc42-depleted cells, the remaining β1 integrin was rarely localized in protrusions (Fig. 7, C and D). The reduction in β1 integrin was rescued with siRNA-resistant cDNA encoding Cdc42 (Fig. 7 E and Fig. S4 D). In contrast to β1 integrin, Cdc42 did not affect levels of N-cadherin or CD44 (not depicted), which have previously been reported to regulate cancer cell interaction with ECs (Qi et al., 2005; Wang et al., 2005). Altogether, our results demonstrate that Cdc42 specifically regulates β1 integrin expression.

β1 integrin is the main Cdc42 target required for cancer cell intercalation and TEM

Because Cdc42 regulates β1 integrin levels, we investigated the effect of β1 integrin depletion on cancer cell interaction with ECs. Two different siRNAs efficiently knocked down β1 integrin expression in PC3 cells, as observed by flow cytometry (Fig. 8 A), immunofluorescence, and immunoblotting (Fig. S5, A and B). β1 integrin depletion reduced PC3 cell adhesion to both ECs and fibronectin, and decreased TEM (Fig. 8, B–D). However, β1 integrin depletion had the strongest effect on intercalation, similar to Cdc42 depletion: >50% of β1 integrin-depleted cells still did not intercalate between ECs after 300 min (Fig. 8 E, Fig. S5 C, and Video 6). Most β1 integrin–depleted PC3 cells remained rounded and did not move on top of ECs (Fig. 8 E and Video 6), and we observed some cells blebbing when trying to intercalate (unpublished data). β1 integrin depletion also had a similar phenotype to Cdc42 depletion during cell spreading on fibronectin: β1 integrin–depleted cells extended protrusions in multiple directions, and had reduced or delayed spreading (unpublished data). Importantly, exogenous β1 integrin expression (Fig. S5, D and E) rescued the reduced intercalation of Cdc42-depleted cancer cells, whereas exogenous β1 integrin alone did not increase intercalation (Fig. 8 F). This demonstrates that the decrease in β1 integrin expression induced by Cdc42 depletion is sufficient to explain the defect in cancer cell interaction with ECs and the ECM. β1 integrin regulation by Cdc42 is therefore crucial for cancer cell interaction with ECs.

are magnified in the "zoom" column. Bar, 50 µm. (D) Quantification of β1 integrin localization in F-actin–rich protrusions, $n = 3$. (E) FACS analysis for β1 integrin after Cdc42 depletion and reexpression of a Cdc42-siRNA–resistant-cDNA; $n = 3$. Values are means ± SEM (error bars); *, $P < 0.05$; **, $P < 0.01$; ***, $P < 0.001$. See also Fig. S6.

Cdc42 regulates β1 integrin at the transcriptional level via SRF activation

Because depletion of Cdc42 dramatically decreased β1 integrin protein levels, we tested if it affected β1 integrin transcription. β1 integrin mRNA levels were reduced by nearly 50% after Cdc42 depletion (Fig. 9 A). We used a 3,000-bp region upstream of the β1 integrin ATG to determine whether Cdc42 affected β1 integrin gene expression. Cdc42 depletion reduced the activity of this β1 integrin promoter in PC3 cells (Fig. 9 B). Conversely, expression of wild-type Cdc42 or constitutively active Cdc42-V12 stimulated transcription from the β1 integrin promoter (Fig. 9 C). The SRF/megakaryoblastic leukemia 1 (MAL) transcription factor complex has been reported to regulate β1 integrin transcription (Brandt et al., 2009). Wild-type and constitutively active Cdc42 stimulated the activity of the SRF target c-fos promoter (Fig. 9 D), and Cdc42 depletion reduced the activity of this promoter in PC3 cells (Fig. 9 F). RhoA is well known to stimulate SRF (Hill et al., 1995; Olson and Nordheim, 2010), but Cdc42 did not act via RhoA, as RhoA depletion did not affect Cdc42-induced activation of the β1 integrin promoter (Fig. 9 E). Finally, the depletion of SRF in Cdc42-V12–expressing cells reduced the activity of the β1 integrin promoter, demonstrating that Cdc42 activates the β1 integrin promoter via SRF (Fig. 9 G). Moreover, β1 integrin protein levels were also decreased by SRF depletion in PC3 cells (Fig. 9 H) and Cos7 cells (not depicted).

Expression of SRF-VP16, a constitutively active form of SRF (Hill et al., 1994), rescued the inhibition of PC3 cell intercalation induced by Cdc42 depletion (Fig. 9 I). SRF/MAL activity is known to be increased by stimuli that induce actin polymerization (Olson and Nordheim, 2010), and, interestingly, we noted that Cdc42-depleted cancer cells consistently had lower levels of F-actin (Fig. 7 C and Fig. S4, A and D). Altogether, our results demonstrate that Cdc42 regulates β1 integrin transcription by acting on the SRF signaling pathway, and that this mechanism accounts for the effects of Cdc42 on cancer cell intercalation.

Discussion

In this study, we have investigated the mechanisms underlying the interactions of cancer cells with ECs. We demonstrate that Cdc42 in cancer cells regulates cancer cell TEM by contributing to multiple steps of the extravasation process. Although several Rho GTPases, including Cdc42, contribute to cancer cell adhesion to ECs, Cdc42 is unique in strongly affecting intercalation of cancer cells into the EC monolayer, and in regulating cancer cell spreading on the subendothelial ECM. Interestingly, Cdc42 mediates cancer cell intercalation primarily by regulating β1 integrin expression. In vivo, Cdc42 is also required for cancer cells to spread on ECs and early colonization in the lung. Finally, we demonstrate that the initial transient depletion of Cdc42 is sufficient to inhibit experimental metastasis, indicating that the role of Cdc42 in cancer–EC interaction is important for the metastatic process.

In addition to Cdc42, several other Rho GTPase family members affected cancer cell adhesion to ECs, but only Cdc42 had long-term effects on intercalation. The mechanistic basis of the involvement of the other Rho GTPases during cancer cell adhesion to ECs is currently being investigated; based on our results, at least for RhoA and Rac1, it is unlikely to involve changes to β1 integrin levels. Several Rho proteins are known to affect cancer cell invasion in vitro and in vivo (Vega and Ridley, 2008), but little is known of their roles in the specific step of extravasation. RhoA and RhoC depletion have been reported to increase PC3 cell adhesion to a bone marrow EC cell line, whereas Rac1 and RhoC but not RhoA depletion reduced diapedesis measured in Transwells (Sequeira et al., 2008; van Golen et al., 2008). In contrast, we found that both RhoA and RhoC depletion in PC3 cells reduced adhesion to human umbilical vein ECs (HUVECs). The reasons for these discrepancies are unknown but could be caused by the use of an EC line, whereas we used primary ECs.

Although Cdc42-, Rac1-, or RhoA-depleted cells all had lower adhesion to ECs, only depletion of Cdc42 decreases β1 integrin expression, which then reduces intercalation as well as adhesion and spreading on the subendothelial ECM. β1 integrin has recently been described to regulate contractile forces that facilitate cancer cell invasion within the ECM (Mierke et al., 2011). Thus, any protrusions from Cdc42-depleted cancer cells that do extend between ECs might not attach for long enough to the ECM to sustain EC junction opening. In addition, protrusions on Cdc42-depleted cells show a high level of membrane blebbing, and thus may not be able to provide the sustained mechanical force required to disrupt EC junctions.

We show that Cdc42 regulates β1 integrin expression. Consistent with our results, Cdc42 knockout hematopoietic stem cells were reported to have reduced β1 integrin expression levels (Yang et al., 2007), but the molecular basis for this decrease was not known. We found that Cdc42 regulates β1 integrin transcription through the SRF transcription factor. Although SRF activity is most frequently associated with RhoA, Cdc42 has also been shown to stimulate SRF (Hill et al., 1995). In addition, Vav GEFs were found to induce SRF activation through Cdc42 and Rac1 (Charvet et al., 2002). Recently, β1 integrin expression was shown to be repressed by a novel protein SCA1, which binds to the SRF cofactor MAL (Brandt et al., 2009). SRF was reported to bind to the promoter of the β1 integrin gene (Brandt et al., 2009), and we found that SRF depletion dramatically reduced expression of a β1 integrin promoter in PC3 cells. Cdc42 could affect SRF/MAL activity through regulating G-actin levels (Olson and Nordheim, 2010), as its depletion strongly reduces F-actin levels. Interestingly, in our model, only Cdc42 but not RhoA affects β1 integrin levels, and RhoA was not required for Cdc42 to activate SRF. Cdc42 might therefore activate another transcription factor that acts together with SRF to stimulate β1 integrin gene expression.

Lower β1 integrin levels are likely to contribute to the reduction in cancer cell spreading and protrusion extension that we observed in Cdc42-depleted cells in the lung vasculature. Indeed, β1 integrin has been shown to be required for early entrapment of cancer cells in the lung (Wang et al., 2004) and to be involved in the metastasis process and formation of

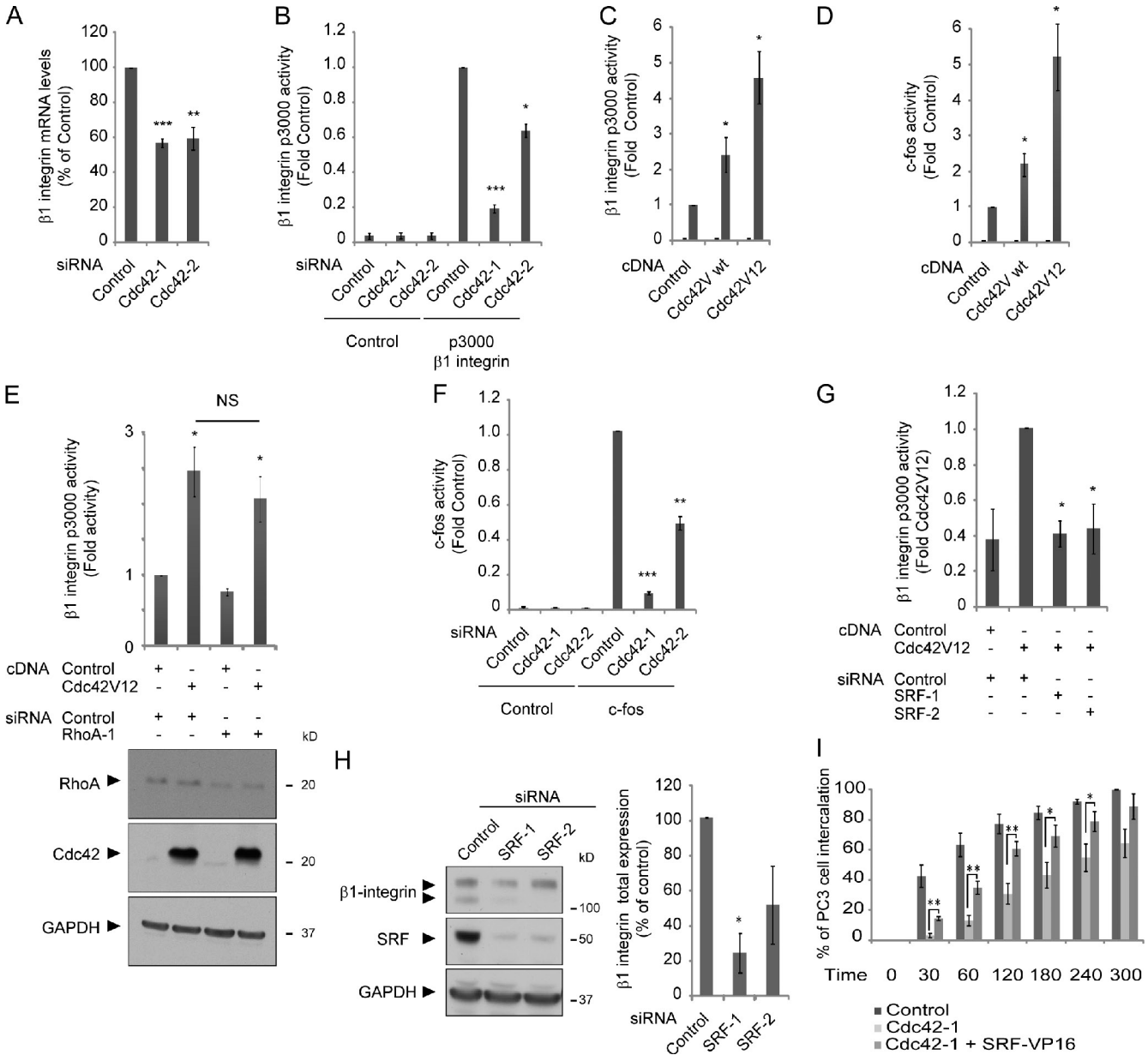

Figure 9. **Cdc42 regulates β1 integrin transcription via SRF.** (A) β1 integrin mRNA levels quantified by quantitative PCR. (B–G) Activities of p3000 β1 integrin and c-fos promoters were assessed by luciferase assays after PC3 cell transfection with the indicated siRNAs (B), Cos7 cell transfection with wild-type or constitutively active Cdc42-V12 (C and D), Cos7 cell transfection with Cdc42-V12 and RhoA siRNAs (E), PC3 cell transfection with the indicated siRNAs (F), and Cos7 cell transfection with SRF siRNAs (G). (H) Lysates of PC3 cells transfected as indicated were immunoblotted for SRF, β1 integrin, and GAPDH (loading control). A representative blot is shown (left) as well as a quantification of three independent blots for β1 integrin (right). (I) Time of intercalation for individual cells, expressed as the percentage of the total cell number. PC3 cells were transfected with SRF-VP16 24 h after siRNA transfection. Values are means ± SEM (error bars; $n = 3$); ***, $P < 0.001$; **, $P < 0.01$; *, $P < 0.05$.

metastatic foci in the lungs in vivo (Wang et al., 2004; Kren et al., 2007; Huck et al., 2010). Interestingly, α3β1 integrin is required for attachment of HT1080 fibrosarcoma cells to laminin exposed in small gaps between ECs in the lung vasculature in vivo (Wang et al., 2004); in a zebrafish model, β1 integrin mediates adhesion of cancer cells to the blood vessel wall (Stoletov et al., 2010).

The reduced levels of β1 integrin could also explain the lower retention of Cdc42-depleted cells in the lung, as β1 integrin provides pro-survival and antiapoptotic signals. Indeed, the β1 integrin–FAK signaling axis controls the initial proliferation of micrometastases in the lung (Shibue and Weinberg, 2009). Recent evidence shows that interfering with cancer cell attachment and spreading by inhibiting β1 integrin sensitizes tumor cells to TRAIL-induced apoptosis (Phipps et al., 2011). It is thus possible that Cdc42 depletion similarly decreases resistance to apoptotic signals induced by immune cells present in severe combined immunodeficiency (SCID) mice such as natural killer cells, which contribute to antitumoral protection in the lungs (Yang et al., 2006).

Cdc42 is well known to regulate cancer cell invasion in vitro and is overexpressed in several human tumor types

(Vega and Ridley, 2008; Stengel and Zheng, 2011), but so far its effects on tumor growth and metastasis in vivo can be explained by changes in cell proliferation (Bouzahzah et al., 2001; Hua et al., 2011). It is therefore particularly interesting that, in our studies, transient depletion of Cdc42 at a critical step of the metastatic cascade was sufficient to reduce metastatic foci after 6 wk. In vitro, Cdc42 depletion in PC3 cells did not affect proliferation or cell division (unpublished data). It is possible that Cdc42-depleted cancer cells initially grow slower than control cells in vivo because of reduced β1 integrin signaling. However, because we injected PC3 cells 3 d after their transfection with siRNA to Cdc42, and the levels of Cdc42 and β1 integrin expression are close to normal 6 d after transfection, our data clearly indicate that Cdc42-induced reduction of cancer cell interaction with ECs in the first 24 h after entry into blood vessels decreases the efficiency of metastasis. Targeting Cdc42 would potentially affect cancer cell–EC interactions for multiple tumor types, whereas targeting cell adhesion molecules on the surface of cancer cells or ECs is more tumor type–specific (Madsen and Sahai, 2010). Interestingly, we have observed in vitro that depletion of Cdc42 in adherent PC3 cells induced their de-adhesion (unpublished data). Delivering Cdc42 inhibitors directly in the blood could therefore block the interaction of cancer cells to vessel walls, or help to detach already attached cancer cells, and hence reduce metastasis. Importantly, Cdc42 is not required for T cell TEM (Heasman et al., 2010) and thus is a potentially selective target to inhibit cancer cell metastasis without affecting leukocyte trafficking.

Materials and methods

Cell culture and reagents

Primary HUVECs were maintained in EBM2 medium (Lonza) on dishes coated with 10 µg/ml fibronectin (Sigma-Aldrich). PC3 and DU145 were cultivated in RPMI-1640 medium supplemented with 10% FCS, 2 mM glutamine, 100 U/ml penicillin, and 50 µg/ml streptomycin. MDA-MB-231 and Cos7 cells were cultivated in DMEM medium supplemented with 10% FCS, 2 mM glutamine, 100 U/ml penicillin, and 50 µg/ml streptomycin. Stable CFP- and YFP-expressing PC3 cells were generated by transfection either with CFP or YFP in CB6 plasmids, respectively, using Lipofectamine 2000 (Invitrogen) according to the manufacturer's instructions. An XTT assay was used to determine cell number and cell viability (Roche).

The following antibodies were used: RhoA (clone 26C4; Santa Cruz Biotechnology, Inc.), Rac1 (EMD Millipore), Cdc42 (clone B-8; Santa Cruz Biotechnology, Inc.), VE-cadherin (clone 75; BD), PECAM-1 (clone JC70A; Dako), PE-conjugated PECAM-1 (clone 390; BioLegend), β-catenin (Sigma-Aldrich), β1 integrin 4B7 (Abcam), β1 integrin 18/CD29 (BD), β1 integrin P4G11 (EMD Millipore), β1 integrin 12G10 (Abcam), β2 integrin P4H9 (EMD Millipore), β3 integrin 25E11 (EMD Millipore), β4 integrin ASC-9 (EMD Millipore), N-cadherin (Abcam), CD44 E4 (provided by I. Dransfield, University of Edinburgh, Edinburgh, UK), Nectin-2 477 (provided by M. Lopez, Marseille, France), SRF (clone G-20; Santa Cruz Biotechnology, Inc.), and GAPDH (EMD Millipore). HRP-conjugated antibodies (GE Healthcare) were detected with chemiluminescence reagent (Thermo Fisher Scientific). Cells were labeled with 2 µM 5-(and-6)-carboxyfluorescein diacetate succinimidyl ester (CFSE; Molecular Probes). Alexa Fluor 546– or TRITC-labeled phalloidin (1:400; Invitrogen) were used to detect F-actin.

Cell transfection and Western blotting

All siRNAs (Thermo Fisher Scientific) are single oligos (Table S1). PC3 cells (1.25×10^5) were plated and transfected after 24 h with individual oligos (100 nM) with Optimem-I and Oligofectamine (Invitrogen). After 72 h, cells were detached from culture plates with nonenzymatic cell dissociation solution (Sigma-Aldrich) and used for functional assays as described previously. For Western blotting, cells were lysed by scraping into sample buffer (NuPAGE 4× SDS sample buffer; Invitrogen), then proteins were separated using precast NuPAGE 4–12% Bis-Tris gels (Invitrogen), transferred to nitrocellulose membrane (Immobilon), and incubated with antibodies in Tris-buffered saline containing 5% nonfat milk and 0.1% Tween-20.

Immunofluorescence

HUVECs were grown to confluency on 13-mm-diameter glass coverslips. CFSE-labeled PC3 cells (2.5×10^4) were added and were fixed at different time points with 3.7% paraformaldehyde in PBS for 20 min. Cells were permeabilized with 0.1% Triton X-100 for 5 min at 4°C and then blocked with 5% FCS in PBS for 20 min. Samples were incubated with primary antibodies for 60 min and then appropriate secondary antibodies (Molecular Probes) or dyes. Samples were mounted onto slides with mounting medium (Dako), and images acquired using a confocal microscope (510 LSM; Carl Zeiss) with a 40× objective lens and Zen software (Carl Zeiss). Images were processed using Photoshop software (Adobe).

Flow cytometry

PC3 cells were transfected with the appropriate siRNAs. After 72 h, 2×10^5 cells were resuspended and incubated with the indicated antibodies and then with Alexa Fluor 488–labeled goat anti–mouse antibody. Samples were analyzed using a flow cytometer (FACSCalibur) and Cell Quest Pro (Software; both from BD) and processed using Flow Jo software.

Luciferase assay

Luciferase assays were performed as specified by the manufacturer (Promega). In brief, PC3 cells were transfected with siRNAs targeting Cdc42 or with control siRNA, and after 48 h were transfected with the different reporter genes. Cos7 cells were transfected with different cDNAs (control, Cdc42, Cdc42-V12, SRF-VP16), and for siRNA experiments were also transfected again 24 h later with single siRNAs targeting SRF or control siRNA, then transfected again with the different reporter genes. PC3 cells and Cos7 cells were maintained in growth medium containing 10% FCS, and luciferase assays were performed 24 h after reporter gene transfection. c-fos and β1 integrin (containing the 3,000 bp upstream of the ATG start codon) reporter genes were provided by D. Brandt and R. Grosse (University of Marburg, Marburg, Germany).

Adhesion assay

CFSE-labeled PC3 cells (2×10^4) were added to confluent HUVECs in 96-well plates for 15 min at 37°C, then washed once with PBS containing calcium and magnesium. Each condition was performed at least in triplicate. Adherent cells were quantified with a Fusion α-FP plate reader (PerkinElmer). Fusion 4.02 software and Microsoft Excel were used to acquire raw data and process them, respectively. Adhesion to fibronectin (10 µg/ml; Sigma-Aldrich)- and Matrigel (100 µg/ml; BD)-coated or uncoated plastic was quantified similarly.

TEM assay

HUVECs (5×10^4/well) were plated onto 10 µg/ml fibronectin-coated Costar Transwells (8-µm pore size and 6.5-mm diameter). After 24 h, 2.5×10^4 CFSE-labeled PC3 cells were added. 40 ng/ml HGF was added as a chemo-attractant in the lower chamber. After 8 h at 37°C, PC3 cells were recovered from the bottom of the filter, resuspended in PBS containing 5% FCS, and counted by flow cytometry (FACSCalibur 3.7; BD). Results were processed using Cell Quest software. The 3D TEM assay, using HUVECs plated on a layer of Collagen-I, was carried out as described previously (Cain et al., 2011).

Time-lapse microscopy

CFSE-labeled PC3 cells (3×10^4) were added to confluent HUVECs on 24-well plates. Cells were monitored by time-lapse microscopy for up to 5 h in a humidified chamber at 37°C and 5% CO_2 with an inverted microscope (TE2000; Nikon) equipped with a motorized stage (Prior Scientific), with a 10× or a 20× objective lens and using MetaMorph software (Molecular Devices). Cells were tracked manually using ImageJ software. To quantify intercalation, a cell was considered as intercalated when its shape was not round, when it was no longer phase-bright, and when it was clearly part of the EC monolayer.

To determine spread area, cells plated on 10 µg/ml fibronectin were imaged by time-lapse microscopy for 1 h, and the spread area of >100 cells acquired in each of three independent experiments was measured using ImageJ software.

Visualization of cancer cell attachment in lung blood vessels

We used an established technique to observe and image fluorescently labeled tumor cells and capillary ECs in situ in isolated, ventilated blood-free lungs of SCID mice (6–8-wk-old females) by confocal microscopy, as previously described (Im et al., 2004). YFP-PC3 cells were transfected with a control siRNA, and CFP-PC3 cells were transfected with a Cdc42-specific siRNA, or vice versa. 72 h after transfection, both populations were injected in the vena cava (10-min time point) or in the tail vein (6 h and 24 h time points) of mice. Blood vessels were stained with a PE-conjugated mouse anti–PECAM-1 antibody injected in the vena cava 5 min before the animals were sacrificed. Images of PC3 cells and vascular lung ECs were acquired using a confocal microscope (LSM710; Carl Zeiss) at 405 nm (CFP), 488 nm (YFP), and 543 nm (TRITC) with a 20× (quantification experiments) or a 40× (morphology experiments) objective lens. The morphological analysis was performed only on single cells or groups of two cells. 2D and 3D images were processed using Photoshop (Adobe), Amira (VSG), and Volocity (PerkinElmer) software.

A custom algorithm was used to analyze the intensity of the endothelial PECAM-1 staining surrounding cancer cells. First, the cell image was thresholded (with a user-selected threshold). The image was then median filtered using a circle of radius 3, and any "holes" in the cell (dark areas that were completely surrounded by white areas) were filled. To find the pixels surrounding the cell, this image was then dilated (again using a circle of radius 3), and the pixels that were white in the dilated image but not the filled image were selected. To find the pixels inside the cell, the filled image was eroded with a circle with a radius of 1.9. The ratio of the mean value of those pixels in the vessel image corresponding to the surrounding image and corresponding to the inside of the cell was calculated.

Lung metastasis assay

PC3 or MDA-MB-231 cells were transfected with siRNAs. After 72 h, cells were detached from culture plates by incubation in a mild resuspension buffer (Sigma-Aldrich), and 10^6 cells exhibiting 90% viability were suspended in 200 µl of serum-free RPMI before injection into the tail veins of SCID mice (6–8-wk-old female mice). After 4 (MDA-MB-231) or 6 wk (PC3), lungs were fixed and analyzed for the presence of surface metastatic foci. Lung sections were then hematoxylin and eosin stained and scanned (Aperio scanner), and the tumor-covered areas were quantified with the Aperio software.

Statistical analysis

Each condition was performed in triplicate, and experiments were all performed at least three times. Data are expressed as means ± SEM. Statistical significance of in vitro assays was determined by an unpaired Student's *t* test. For 3D ex vivo analysis, at least 50 cells per condition were analyzed with at least three animals per condition. Statistical significance of in vivo assays was determined by a two-way ANOVA test. In all analyses, differences were considered statistically significant at $P < 0.05$.

Online supplemental material

Fig. S1 shows that Cdc42 regulates cancer cell–EC intercalation and transmigration in DU145 and MDA-MB-231 cells. Fig. S2 shows that Cdc42-, Rac1-, and RhoA-siRNA resistant cDNA transfection rescues morphological depletion phenotypes. Fig. S3 shows that Cdc42 depletion reduces cancer cell spreading on lung blood vessels in vivo and experimental metastasis. Fig. S4 shows that Cdc42 but not Rac1 or RhoA regulates β1 integrin cell surface levels. Fig. S5 shows β1 integrin depletion in PC3 cells. Table S1 lists cancer cell lines tested for adhesion to and intercalation between ECs. Table S2 lists siRNA oligos used in experiments. Video 1 shows that Cdc42, Rac1, or RhoA depletion delays cancer cell intercalation. Video 2 shows that Cdc42 depletion reduces cancer cell adhesion to ECs. Video 3 shows that Cdc42 regulates cancer cell adhesion and spreading to fibronectin. Video 4 shows that PC3 cells spread on vascular lung ECs in vivo. Video 5 shows that Cdc42 controls cancer cell spreading on vascular lung ECs in vivo. Video 6 shows that β1 integrin regulates cancer cell interaction with ECs. Online supplemental material is available at http://www.jcb.org/cgi/content/full/jcb.201205169/DC1.

We thank D. Brandt and R. Grosse for luciferase assay constructs, P. Bhavsar for analysis of Rho GTPase expression in PC3 cells, D. Soong for microscopy assistance, and F. Calhabeu, A. Ivetic, M. Parsons, P. Morton, V. Sanz-Moreno, and members of A.J. Ridley's laboratory for helpful discussions.

This work was supported by Cancer Research UK, the Biotechnology and Biological Sciences Research Council, Breast Cancer Campaign, King's College London British Heart Foundation Centre of Excellence, the Association for International Cancer Research, and the Bettencourt-Schueller Foundation. N. Reymond was supported in part by a European Molecular Biology Organization (EMBO) long-term fellowship, B. Borda A'gua by a Graduate Program in Areas of Basic and Applied Biology (GABBA) PhD scholarship (Portugal), and S. Cox by a Royal Society University Research Fellowship.

Submitted: 25 May 2012
Accepted: 12 October 2012

References

Al-Mehdi, A.B., K. Tozawa, A.B. Fisher, L. Shientag, A. Lee, and R.J. Muschel. 2000. Intravascular origin of metastasis from the proliferation of endothelium-attached tumor cells: a new model for metastasis. *Nat. Med.* 6:100–102. http://dx.doi.org/10.1038/71429

Bouzahzah, B., C. Albanese, F. Ahmed, F. Pixley, M.P. Lisanti, J.D. Segall, J. Condeelis, D. Joyce, A. Minden, C.J. Der, et al. 2001. Rho family GTPases regulate mammary epithelium cell growth and metastasis through distinguishable pathways. *Mol. Med.* 7:816–830.

Brandt, D.T., C. Baarlink, T.M. Kitzing, E. Kremmer, J. Ivaska, P. Nollau, and R. Grosse. 2009. SCAI acts as a suppressor of cancer cell invasion through the transcriptional control of β1-integrin. *Nat. Cell Biol.* 11:557–568. http://dx.doi.org/10.1038/ncb1862

Cain, R.J., B.B. d'Água, and A.J. Ridley. 2011. Quantification of transendothelial migration using three-dimensional confocal microscopy. *Methods Mol. Biol.* 769:167–190. http://dx.doi.org/10.1007/978-1-61779-207-6_12

Charras, G., and E. Paluch. 2008. Blebs lead the way: how to migrate without lamellipodia. *Nat. Rev. Mol. Cell Biol.* 9:730–736. http://dx.doi.org/10.1038/nrm2453

Charvet, C., P. Auberger, S. Tartare-Deckert, A. Bernard, and M. Deckert. 2002. Vav1 couples T cell receptor to serum response factor-dependent transcription via a MEK-dependent pathway. *J. Biol. Chem.* 277:15376–15384. http://dx.doi.org/10.1074/jbc.M111627200

Dubin-Thaler, B.J., J.M. Hofman, Y. Cai, H. Xenias, I. Spielman, A.V. Shneidman, L.A. David, H.G. Döbereiner, C.H. Wiggins, and M.P. Sheetz. 2008. Quantification of cell edge velocities and traction forces reveals distinct motility modules during cell spreading. *PLoS ONE.* 3:e3735. http://dx.doi.org/10.1371/journal.pone.0003735

Friedl, P., and S. Alexander. 2011. Cancer invasion and the microenvironment: plasticity and reciprocity. *Cell.* 147:992–1009. http://dx.doi.org/10.1016/j.cell.2011.11.016

Gassmann, P., J. Haier, K. Schlüter, B. Domikowsky, C. Wendel, U. Wiesner, R. Kubitza, R. Engers, S.W. Schneider, B. Homey, and A. Müller. 2009. CXCR4 regulates the early extravasation of metastatic tumor cells in vivo. *Neoplasia.* 11:651–661.

Hall, A. 2009. The cytoskeleton and cancer. *Cancer Metastasis Rev.* 28:5–14. http://dx.doi.org/10.1007/s10555-008-9166-3

Heasman, S.J., L.M. Carlin, S. Cox, T. Ng, and A.J. Ridley. 2010. Coordinated RhoA signaling at the leading edge and uropod is required for T cell transendothelial migration. *J. Cell Biol.* 190:553–563. http://dx.doi.org/10.1083/jcb.201002067

Hill, C.S., J. Wynne, and R. Treisman. 1994. Serum-regulated transcription by serum response factor (SRF): a novel role for the DNA binding domain. *EMBO J.* 13:5421–5432.

Hill, C.S., J. Wynne, and R. Treisman. 1995. The Rho family GTPases RhoA, Rac1, and CDC42Hs regulate transcriptional activation by SRF. *Cell.* 81:1159–1170. http://dx.doi.org/10.1016/S0092-8674(05)80020-0

Hua, K.T., C.T. Tan, G. Johansson, J.M. Lee, P.W. Yang, H.Y. Lu, C.K. Chen, J.L. Su, P.B. Chen, Y.L. Wu, et al. 2011. N-α-acetyltransferase 10 protein suppresses cancer cell metastasis by binding PIX proteins and inhibiting Cdc42/Rac1 activity. *Cancer Cell.* 19:218–231. http://dx.doi.org/10.1016/j.ccr.2010.11.010

Huck, L., S.M. Pontier, D.M. Zuo, and W.J. Muller. 2010. beta1-integrin is dispensable for the induction of ErbB2 mammary tumors but plays a critical role in the metastatic phase of tumor progression. *Proc. Natl. Acad. Sci. USA.* 107:15559–15564. http://dx.doi.org/10.1073/pnas.1003034107

Humphries, M.J. 2000. Integrin structure. *Biochem. Soc. Trans.* 28:311–339. http://dx.doi.org/10.1042/0300-5127:0280311

Im, J.H., W. Fu, H. Wang, S.K. Bhatia, D.A. Hammer, M.A. Kowalska, and R.J. Muschel. 2004. Coagulation facilitates tumor cell spreading in the pulmonary vasculature during early metastatic colony formation. *Cancer Res.* 64:8613–8619. http://dx.doi.org/10.1158/0008-5472.CAN-04-2078

Isaji, T., Y. Sato, T. Fukuda, and J. Gu. 2009. N-glycosylation of the I-like domain of β1 integrin is essential for β1 integrin expression and biological

function: identification of the minimal N-glycosylation requirement for α5β1. *J. Biol. Chem.* 284:12207–12216. http://dx.doi.org/10.1074/jbc.M807920200

Joyce, J.A., and J.W. Pollard. 2009. Microenvironmental regulation of metastasis. *Nat. Rev. Cancer*. 9:239–252. http://dx.doi.org/10.1038/nrc2618

Kren, A., V. Baeriswyl, F. Lehembre, C. Wunderlin, K. Strittmatter, H. Antoniadis, R. Fässler, U. Cavallaro, and G. Christofori. 2007. Increased tumor cell dissemination and cellular senescence in the absence of β1-integrin function. *EMBO J.* 26:2832–2842. http://dx.doi.org/10.1038/sj.emboj.7601738

Kusama, T., M. Mukai, M. Tatsuta, H. Nakamura, and M. Inoue. 2006. Inhibition of transendothelial migration and invasion of human breast cancer cells by preventing geranylgeranylation of Rho. *Int. J. Oncol.* 29:217–223.

Liu, A.Y. 2000. Differential expression of cell surface molecules in prostate cancer cells. *Cancer Res.* 60:3429–3434.

Madsen, C.D., and E. Sahai. 2010. Cancer dissemination—lessons from leukocytes. *Dev. Cell*. 19:13–26. http://dx.doi.org/10.1016/j.devcel.2010.06.013

Margadant, C., M. Kreft, D.J. de Groot, J.C. Norman, and A. Sonnenberg. 2012. Distinct Roles of Talin and Kindlin in Regulating Integrin α5β1 Function and Trafficking. *Curr. Biol.* 22:1554–1563. http://dx.doi.org/10.1016/j.cub.2012.06.060

Martin, M.D., G.J. Kremers, K.W. Short, J.V. Rocheleau, L. Xu, D.W. Piston, L.M. Matrisian, and D.L. Gorden. 2010. Rapid extravasation and establishment of breast cancer micrometastases in the liver microenvironment. *Mol. Cancer Res.* 8:1319–1327. http://dx.doi.org/10.1158/1541-7786.MCR-09-0551

Mehlen, P., and A. Puisieux. 2006. Metastasis: a question of life or death. *Nat. Rev. Cancer*. 6:449–458. http://dx.doi.org/10.1038/nrc1886

Mierke, C.T., B. Frey, M. Fellner, M. Herrmann, and B. Fabry. 2011. Integrin α5β1 facilitates cancer cell invasion through enhanced contractile forces. *J. Cell Sci.* 124:369–383. http://dx.doi.org/10.1242/jcs.071985

Nguyen, D.X., P.D. Bos, and J. Massagué. 2009. Metastasis: from dissemination to organ-specific colonization. *Nat. Rev. Cancer*. 9:274–284. http://dx.doi.org/10.1038/nrc2622

Norman, L.L., J. Brugués, K. Sengupta, P. Sens, and H. Aranda-Espinoza. 2010. Cell blebbing and membrane area homeostasis in spreading and retracting cells. *Biophys. J.* 99:1726–1733. http://dx.doi.org/10.1016/j.bpj.2010.07.031

Olson, E.N., and A. Nordheim. 2010. Linking actin dynamics and gene transcription to drive cellular motile functions. *Nat. Rev. Mol. Cell Biol.* 11:353–365. http://dx.doi.org/10.1038/nrm2890

Phipps, L.E., S. Hino, and R.J. Muschel. 2011. Targeting cell spreading: a method of sensitizing metastatic tumor cells to TRAIL-induced apoptosis. *Mol. Cancer Res.* 9:249–258. http://dx.doi.org/10.1158/1541-7786.MCR-11-0021

Qi, J., N. Chen, J. Wang, and C.H. Siu. 2005. Transendothelial migration of melanoma cells involves N-cadherin-mediated adhesion and activation of the beta-catenin signaling pathway. *Mol. Biol. Cell*. 16:4386–4397. http://dx.doi.org/10.1091/mbc.E05-03-0186

Reymond, N., P. Riou, and A.J. Ridley. 2012. Rho GTPases and cancer cell transendothelial migration. *Methods Mol. Biol.* 827:123–142. http://dx.doi.org/10.1007/978-1-61779-442-1_9

Ridley, A.J. 2011. Life at the leading edge. *Cell*. 145:1012–1022. http://dx.doi.org/10.1016/j.cell.2011.06.010

Sequeira, L., C.W. Dubyk, T.A. Riesenberger, C.R. Cooper, and K.L. van Golen. 2008. Rho GTPases in PC-3 prostate cancer cell morphology, invasion and tumor cell diapedesis. *Clin. Exp. Metastasis*. 25:569–579. http://dx.doi.org/10.1007/s10585-008-9173-3

Shibue, T., and R.A. Weinberg. 2009. Integrin beta1-focal adhesion kinase signaling directs the proliferation of metastatic cancer cells disseminated in the lungs. *Proc. Natl. Acad. Sci. USA*. 106:10290–10295. http://dx.doi.org/10.1073/pnas.0904227106

Stengel, K., and Y. Zheng. 2011. Cdc42 in oncogenic transformation, invasion, and tumorigenesis. *Cell. Signal.* 23:1415–1423. http://dx.doi.org/10.1016/j.cellsig.2011.04.001

Stoletov, K., H. Kato, E. Zardouzian, J. Kelber, J. Yang, S. Shattil, and R. Klemke. 2010. Visualizing extravasation dynamics of metastatic tumor cells. *J. Cell Sci.* 123:2332–2341. http://dx.doi.org/10.1242/jcs.069443

van Golen, K.L., C. Ying, L. Sequeira, C.W. Dubyk, T. Reisenberger, A.M. Chinnaiyan, K.J. Pienta, and R.D. Loberg. 2008. CCL2 induces prostate cancer transendothelial cell migration via activation of the small GTPase Rac. *J. Cell. Biochem.* 104:1587–1597. http://dx.doi.org/10.1002/jcb.21652

Vega, F.M., and A.J. Ridley. 2007. SnapShot: Rho family GTPases. *Cell*. 129:1430.e1–1430.e2. http://dx.doi.org/10.1016/j.cell.2007.06.021

Vega, F.M., and A.J. Ridley. 2008. Rho GTPases in cancer cell biology. *FEBS Lett.* 582:2093–2101. http://dx.doi.org/10.1016/j.febslet.2008.04.039

Wang, H., W. Fu, J.H. Im, Z. Zhou, S.A. Santoro, V. Iyer, C.M. DiPersio, Q.C. Yu, V. Quaranta, A. Al-Mehdi, and R.J. Muschel. 2004. Tumor cell α3β1 integrin and vascular laminin-5 mediate pulmonary arrest and metastasis. *J. Cell Biol.* 164:935–941. http://dx.doi.org/10.1083/jcb.200309112

Wang, H.S., Y. Hung, C.H. Su, S.T. Peng, Y.J. Guo, M.C. Lai, C.Y. Liu, and J.W. Hsu. 2005. CD44 cross-linking induces integrin-mediated adhesion and transendothelial migration in breast cancer cell line by up-regulation of LFA-1 (α L β2) and VLA-4 (α4β1). *Exp. Cell Res.* 304:116–126. http://dx.doi.org/10.1016/j.yexcr.2004.10.015

Yang, Q., S.R. Goding, M.E. Hokland, and P.H. Basse. 2006. Antitumor activity of NK cells. *Immunol. Res.* 36:13–25. http://dx.doi.org/10.1385/IR:36:1:13

Yang, L., L. Wang, H. Geiger, J.A. Cancelas, J. Mo, and Y. Zheng. 2007. Rho GTPase Cdc42 coordinates hematopoietic stem cell quiescence and niche interaction in the bone marrow. *Proc. Natl. Acad. Sci. USA*. 104:5091–5096. http://dx.doi.org/10.1073/pnas.0610819104